SANDWICH COMPOSITES SKIN PANEL OPTIMIZATION FOR THE COMMON RESEARCH MODEL WING

Yasser M. Meddaikar[1], Johannes K.S. Dillinger[2], Wolf R. Krüger[2], Roeland De Breuker[3], Gustavo H. C. Silva[1], Pedro Higino Cabral[4] & Alex Pereira do Prado[4]

[1]former DLR - Institute of Aeroelasticity, Bunsenstrasse 10, 37073 Göttingen, Germany
[2]DLR - Institute of Aeroelasticity, Bunsenstrasse 10, 37073 Göttingen, Germany
[3]Delft University of Technology, 2629HS, Delft, The Netherlands
[4]Embraer S.A., São José dos Campos, 12227-901 São Paulo, Brazil

Abstract

This paper presents an approach for optimizing practical commercial-scale aircraft wings using sandwich composites in a preliminary design stage. The approach uses lamination parameters as design variables in a continuous optimization step. Structural constraints for classic composite laminate design such as material failure and buckling, and for sandwich design such as crimping, wrinkling, dimpling and core shear failure are accounted for using industrial-standard and empirical methods driven by finite element analyses. As an application case, optimization studies are performed at a skin panel level on the open-source Common Research Model (CRM) wing. Optimization trends show areas of the wingbox where sandwich composites offer superior structural performance, as well as potential cost savings by requiring lesser number of stringers. The aim and novelty of this work is to present performance gains that can be achieved using sandwich composites in primary load-carrying aircraft structures when compared with monolithic composite designs and through this, to provide a motivation for further research and development in sandwich composites and their applications.

Keywords: composite optimization; sandwich; lamination parameter; common research model

1. Introduction

Over the last few decades the aerospace industry has seen a steady increase in use of composite materials. The superior mechanical properties of composites, ability to tailor their properties efficiently and possible lower manufacturing costs due to integration of parts has been a major reason for this increased focus on its research and application.

The present trend of aircraft wings show designs that are dominated by stiffness requirements when compared to strength requirements [1], especially in the upper skin. Moreover, outer sections of the wing are sized due to minimum gauge requirements arising out of handling and manufacturing needs. With advancements in materials beyond carbon-fibre T300 and IM7, designers can only expect strength requirements to be further overshadowed by stiffness and handling requirements.

The advantages of sandwich composites have been known since their invention in the 1960s. Practical experience shows that their benefits come alongside a number of unique engineering challenges, which must be carefully considered in realistic designs [2]. The potential advantages and challenges have motivated a wide range of research covering topics such as characterization of failure modes [3, 4, 5], development of modelling strategies [6, 7] and on optimization of sandwich composites [8, 9, 10, 11, 12, 13, 14, 15, 16, 17, 18, 19] to name a few.

The present work is a condensed form of a recently published work [19] on a design approach suited for a preliminary design stage towards the optimization of large-scale wingbox structures using sandwich composites. The approach can be used to make trend studies to gauge any potential performance benefits that sandwich composites can offer when compared to classical monolithic composites. For the optimization studies , the NASA Common Research Model (CRM) [20] is chosen,

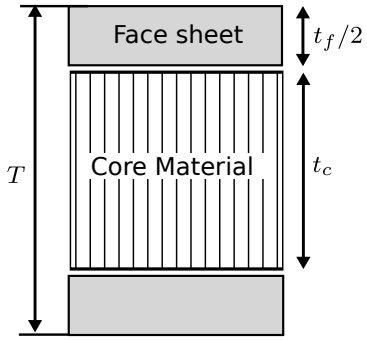

Figure 1 – Cross-section of a classic sandwich composite.

specifically a structural model of the CRM wing generated at the DLR - Institute of Aeroelasticity [21], under the configuration name FERMAT.
The present paper is organized as follows. Section 2 introduces the different failures modes in sandwich composites and how they have been addressed in the present work. The applied optimization strategy is detailed in Section 3. The skin panel problem of the CRM wing is presented in Section 4. together with a summary of the optimization objective and constraints. The results from the optimization study are discussed in Section 5 followed by a conclusion of and outlook based on the presented work.

2. Addressing Failure Modes of Sandwich Composites

In a typical preliminary-stage wing optimization [22, 1], structural constraints such as strength failure and buckling instability are considered for classic monolithic composite designs. Sandwich composites are susceptible to other failure mechanisms as listed in the Composite Materials Handbook Volume-6 [23] (CMH-17) and illustrated in Figure 2. These failure modes are conservatively accounted for in the CMH-17 using either analytical or empirical expressions. The approach presented in this paper aims to use such conservative estimates to make performance studies suited to a preliminary stage of wing design.
The first two failure modes (a) - (b) in Figure 2, facesheet or material failure and buckling are common to both monolithic and sandwich composite design. The sandwich-specific failure modes (c) - (g) are accounted for using formulae in the CMH-17 [23]. The remaining failure modes (h) - (k) are usually considered in a later detailed design phase or are loading conditions that are not common to wingbox type applications and are hence not considered in this preliminary-stage design study.

2.1 Failure modes for both monolithic and sandwich composites

Facesheet/Laminate failure

In this paper, laminate or facesheet failure is determined using a common technique employed in industry known as the Angle Minus Longitudinal (AML) method [24]. AML refers to the percentage of $\pm 45^\circ$ plies (angle) minus the percentage of plies at 0° (longitudinal), a metric for which laminates of similar values tend to possess the same failure modes in notched or damaged compression tests. Open-hole compression tests (OHC), as shown in Figure 5, can then be used as a direct laminate-level empirical strain allowable. For this criteria, only the face sheet thickness and its layup angles need to be known.

Buckling instability

Structural instability due to buckling is solved as an eigenvalue problem using the buckling solver in MSC.NASTRAN [25].

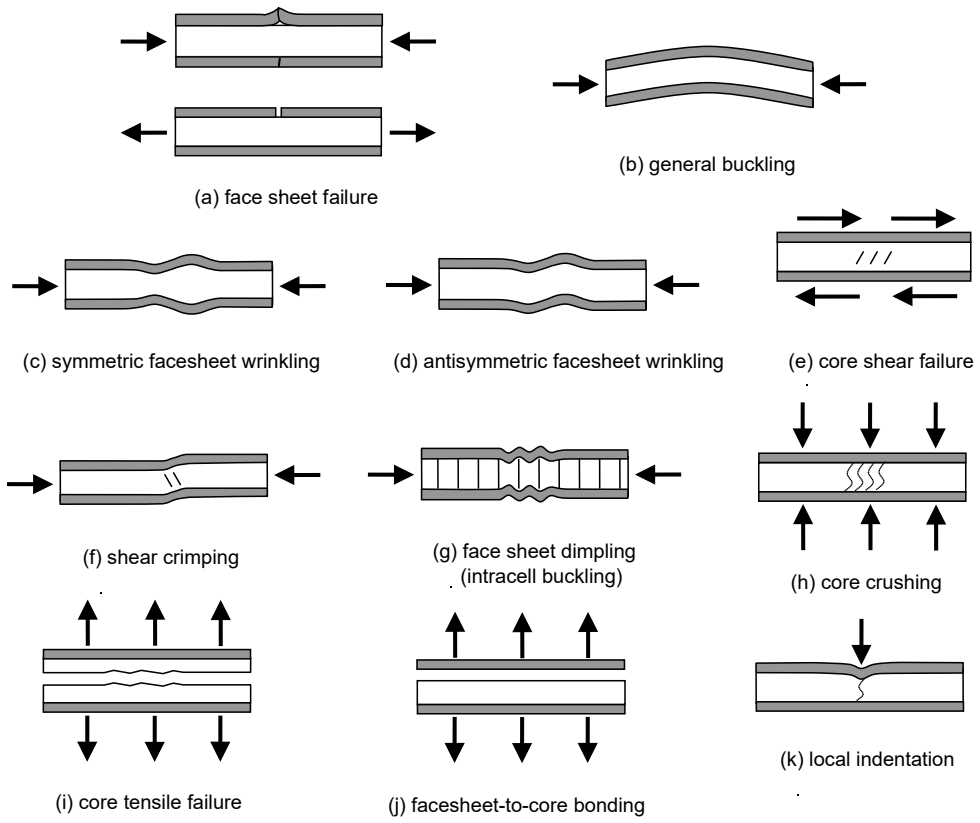

Figure 2 – Failure modes of sandwich composites [23].

2.2 Failure modes only for sandwich composites

Facesheet wrinkling

Facesheet wrinkling is a local instability mode where the facesheet buckles with a characteristic wavelength being of the order of magnitude as the thickness of the core. Sandwich structures with thin facesheets and light cores are susceptible to this failure mode. For sandwich composites with honeycomb type of cores, wrinkling stress is given by the following relations,

$$\sigma_{wrink} = C_1 (E_f E_c G_c)^{1/3} + C_2 G_c \frac{t_c}{t_f} \tag{1}$$

$$\sigma_{wrink} = C_3 \sqrt{\frac{t_f}{t_c} E_c E_f} + C_4 G_c \frac{t_c}{t_f} \tag{2}$$

Eqs. 1 and 2 are applicable when the sandwich is considered to have a thick or thin core respectively, where the definition of a sandwich with thick core is determined by the following expression

$$t_c \geq 1.82 t_f \sqrt[3]{\frac{E_f E_c}{G_c^2}} \tag{3}$$

The coefficients C_1 - C_4 are generally adapted to experimental results and a wide range of values have been reported, for instance [26, 27, 28]. Conservative values of $C_1 = 0.247$, $C_2 = 0.078$, $C_3 = 0.33$, $C_4 = 0$ are suggested in the CMH-17.

Shear crimping

Shear crimping is an instability mode that occurs due to a low core shear modulus. The facesheet stress at which crimping occurs is given by

$$\sigma_{crimp} = \frac{h^2 G_c}{(2t_f) t_c} \tag{4}$$

where h is the distance between the mid-planes of the upper and lower facesheet.

Facesheet dimpling

Facesheet dimpling or intracell buckling occurs when the facesheet buckles between the cell-walls of a honeycomb core. The facesheet stress at which dimpling occurs is given by

$$\sigma_{dimp} = \frac{1}{t_f}\left(\frac{\pi}{s}\right)^2 \{D_{11} + 2(D_{12} + 2D_{66}) + D_{22}\} \tag{5}$$

Core shear failure

This failure mode occurs due to the core failing in shear. Assuming conservatively that the core carries all of the transverse loads, the transverse shear stress is given by

$$\begin{aligned} \tau_{xz} &= \frac{Q_x}{t_c} \\ \tau_{yz} &= \frac{Q_y}{t_c} \end{aligned} \tag{6}$$

The transverse loads Q_x and Q_y are extracted as forces from a static analysis in MSC.NASTRAN. Failure occurs when the transverse shear stresses are greater than the shear strength of the core material.

In the above Eqs. 1 - 6, the geometric quantities t_c, t_f and s are the thickness of the core, thickness of each facesheet and the cell-size of the honeycomb core respectively. For composite facesheets, the stiffness terms are directionally-dependent - E_f represents the effective bending stiffness of the facesheet in the direction of loading and is calculated from the bending stiffness matrix D. E_c is the core elastic modulus normal to the sandwich facesheets and G_c is the core shear modulus. Honeycomb cores tend to have different properties in their ribbon and transverse directions and as a result, the values G_{xz}, G_{yz} and $\sqrt{G_{xz}G_{yz}}$ are suggested in the CMH-17 to be used in place of G_c, depending on whether the loading is in the X, Y or XY direction. The failure stresses for the above sandwich failure modes are defined for a uniaxial state of compression. Loading states along different directions can be considered by using corresponding values for the directional stiffnesses.

For the sake of convenience, the failure stress in the case of wrinkling, crimping and dimpling are recast as failure strains through the directional in-plane stiffness. In the following sections, the failure criteria of AML, wrinkling, crimping and dimpling are collectively denoted as strain-based failure criteria, while core shear failure is termed a force-based failure criteria.

3. Optimization strategy

The optimization of composite structures has been successfully studied using a commonly-applied two-step approach [29, 30, 31, 32, 33, 34, 35, 1] for a wide range of applications. In the first step, lamination parameters and thickness of the composite are used as design variables. This enables the use of efficient gradient-based optimizers to identify interesting regions in a vast design space and leads to an overall faster convergence in the second step. In the second step, the optimum stiffness design obtained earlier is used as a starting point to obtain an optimal stacking sequence distribution, for instance in [36, 37, 35, 1].

The continuous optimization step is the focus of this paper, in order to perform design studies representative of a preliminary design stage. The design obtained from the continuous optimization represents the theoretical upper-bound in performance achievable for the given material and constraints. In other words, this step results in the optimal stiffness distribution of the structure and is indicative of the structural performance possible.

The optimization problem can be stated as follows,

$$\begin{aligned} \min_{\mathbf{x}} \quad & f(\mathbf{x}) \\ \text{subject to:} \quad & P_j(\mathbf{x}) \leq 1, \quad j = 1...n_p \\ & C_k(\mathbf{x}) \leq 1 \quad k = 1...n_c \\ & x_i^l \leq x_i \leq x_i^u \quad x_i \in \mathbf{x} \end{aligned} \tag{7}$$

The design variables $\mathbf{x}$ comprise of thickness and lamination parameters. The objective function $f(\mathbf{x})$ is to be minimized, structural weight in this case. The physical constraints P which are the failure modes, and the admissibility constraints C on the design variables are normalized such that values less than 1 are feasible.

3.1 Lamination parameters and admissibility constraints

A novel lamination parameters scheme [17] applicable to sandwich composites, or multi-material laminates in general is utilized in this work. This approach is based on the definition of material blocks with an offset in between its two laminate halves.

In the general case of symmetric sandwich composites, where both facesheet and core comprise of anisotropic composite materials, the exact in-plane and bending stiffness matrices are calculated as

$$A = t_c \left[\xi^A\right]_c \{U\}_c + t_f \left[\xi^A\right]_f \{U\}_f \tag{8}$$

$$D = \tfrac{t_c^3}{12} \left[\xi^D\right]_c \{U\}_c + \tfrac{t_f^3}{12} \left[\xi^D\right]_f \{U\}_f + \tfrac{t_c t_f}{4} \left(t_f \left[\xi^{Bu}\right]_f + t_c \left[\xi^A\right]_f\right) \{U\}_f \tag{9}$$

where t is the thickness, U is the matrix of laminate invariants, $\xi^{A,B_u,D}$ are lamination parameters and subscripts f and c denote properties for the facesheet and core respectively. The lamination parameters in the above equations are defined as

$$\xi^A_{[1,2,3,4]} = \frac{1}{2}\int_{-1}^{1} [\cos 2\theta(\bar{z}), \cos 4\theta(\bar{z}), \sin 2\theta(\bar{z}), \sin 4\theta(\bar{z})] d\bar{z} \tag{10}$$

$$\xi^{Bu}_{[1,2,3,4]} = -2\int_{-1}^{0} [\cos 2\theta(\bar{z}), \cos 4\theta(\bar{z}), \sin 2\theta(\bar{z}), \sin 4\theta(\bar{z})] \bar{z} d\bar{z} \tag{11}$$

$$\xi^{Bl}_{[1,2,3,4]} = 2\int_{0}^{1} [\cos 2\theta(\bar{z}), \cos 4\theta(\bar{z}), \sin 2\theta(\bar{z}), \sin 4\theta(\bar{z})] \bar{z} d\bar{z} \tag{12}$$

$$\xi^D_{[1,2,3,4]} = \frac{3}{2}\int_{-1}^{1} [\cos 2\theta(\bar{z}), \cos 4\theta(\bar{z}), \sin 2\theta(\bar{z}), \sin 4\theta(\bar{z})] \bar{z}^2 d\bar{z} \tag{13}$$

The full set of design variables for an optimization in this general case are

$$\mathbf{x} = \left\{ \; t_c \mid \quad t_f \mid \quad \xi^A_c \mid \quad \xi^A_f \mid \quad \xi^{Bu}_f \mid \quad \xi^D_c \mid \quad \xi^D_f \; \right\}^T \tag{14}$$

For sandwich composites containing an isotropic core material with a low stiffness in comparison with the facesheet material, such as in the case of foam or honeycomb cores, the above equations are simplified, resulting in a reduced set of design variables

$$\mathbf{x} = \left\{ \; t_c \mid \quad t_f \mid \quad \xi^A_f \mid \quad \xi^{Bu}_f \mid \quad \xi^D_f \; \right\}^T \tag{15}$$

with the stiffness matrices calculated as

$$A = t_f \left[\xi^A\right]_f \{U\}_f \tag{16}$$

$$D = \tfrac{t_f^3}{12} \left[\xi^D\right]_f \{U\}_f + \tfrac{t_c t_f}{4} \left(t_f \left[\xi^{Bu}\right]_f + t_c \left[\xi^A\right]_f\right) \{U\}_f \tag{17}$$

Depending on the application and the accuracy needed, the lamination parameters ξ^{Bu}_f may be replaced with $\xi^{Bu}_f = 1/2(\xi^A_f + \xi^D_f)$ in Eqs. 9 and 17. This results in a smaller number of lamination parameters, albeit by increasing the inaccuracy of D, which could be acceptable or not depending on the application. In the present study, the full set of lamination parameters is used for the sake of convenience. Details on the lamination parameters, stiffness matrices and accuracies of the different approximations are presented in Silva et al. [17].

Accounting for transverse shear stiffness

Sandwich composites typically have a large thickness and shear deformation effects can no longer be neglected in such a case. The Reissner-Mindlin plate theory is considered in order to account for the transverse shear stiffness. The transverse shear stiffness G is represented [13] in terms of lamination parameters through the material invariants as

$$\{\hat{G}\} = \begin{bmatrix} 1 & \xi_1^A \\ 0 & -\xi_3^A \\ 1 & -\xi_1^A \end{bmatrix} \begin{Bmatrix} U_6 \\ U_7 \end{Bmatrix} \tag{18}$$

$$\{G\} = [T]\{\hat{G}\} \tag{19}$$

in a vectorized form, where $\hat{G}$ is the thickness-normalized transverse shear stiffness matrix and T is the total thickness.
The material invariants are defined as

$$\begin{Bmatrix} U_6 \\ U_7 \end{Bmatrix} = \frac{1}{2} \begin{bmatrix} 1 & 1 \\ 1 & -1 \end{bmatrix} \begin{Bmatrix} Q_{44} \\ Q_{55} \end{Bmatrix} \tag{20}$$

where Q_{44} and Q_{55} are a part of the transverse shear terms in the stress-strain relationship for a transversely isotropic lamina with values being the engineering constants G_{23} and G_{13} respectively.

$$\begin{Bmatrix} \tau_{23} \\ \tau_{13} \end{Bmatrix} = \begin{bmatrix} Q_{44} & 0 \\ 0 & Q_{55} \end{bmatrix} \begin{Bmatrix} \gamma_{23} \\ \gamma_{13} \end{Bmatrix} \tag{21}$$

Admissibility constraints

Admissibility constraints for lamination parameters are chosen as formulated in [38] as

$$\text{Bounds: } -1 \leq \xi_{[1,2,3,4]}^{[A,Bl,Bu,D]} \leq 1 \tag{22}$$

$$\text{Feasibility: For } k = A, B_l, B_u, D,$$

$$2(\xi_1^k)^2 - 1 \leq \xi_2^k \leq 1 - 2(\xi_3^k)^2 \tag{23}$$

$$2(\xi_2^k + 1)(\xi_3^k)^2 - 4\xi_1^k \xi_3^k \xi_4^k + (\xi_4^k)^2 \leq [\xi_2^k - 2(\xi_1^k)^2 + 1](1 - \xi_2^k) \tag{24}$$

More extensive formulations of these constraints exist in literature, however the above form has been utilized on account of its simplicity and the acceptable results attainable [1] in retrieving the stacking sequence in the second step.
Practical design requirements such as the use of standard angles $[0°, \pm 45°, 90°]$, requirement on balanced laminates and angle fractions can be formulated on the lamination parameters as

$$\text{Standard Angles: } \xi_4^{[A,Bl,Bu,D]} = 0 \tag{25}$$

$$\text{Balance: } \xi_3^A = 0 \tag{26}$$

$$\text{Angle Fraction: } v_0 = \frac{\xi_2^A + 2\xi_1^A + 1}{4}, v_{90} = \frac{\xi_2^A - 2\xi_1^A + 1}{4}, v_{\pm 45} = \frac{\pm 2\xi_3^A - \xi_2^A + 1}{4} \tag{27}$$

Further constraints on the lamination parameters such as due to blending [39] can also be included. Since the present paper deals with trend studies at the level of a skin panel, these have not been considered.

3.2 Physical constraints

The failure modes described in Section 2. represent the physical constraints to be satisfied in the optimization. Typically these are cast in the form of inequality constraints for an optimizer

$$r_k^l \leq r_k(\mathbf{x}) \leq r_k^u, r_k \in r(\mathbf{x}) \tag{28}$$

where r_k is some physical response bounded by r_k^l and r_k^u.

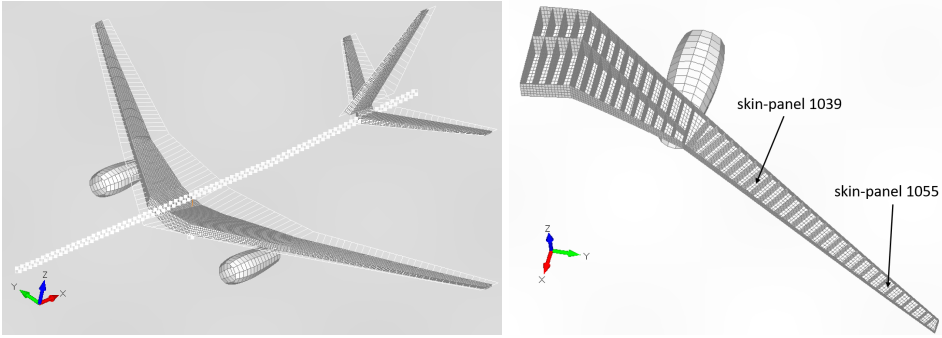

Figure 3 – Structural FE model of the CRM aircraft (FERMAT [21]), left plot, and wing (without upper skin for visualization), right plot.

Failure modes such as buckling are included as lower bounds on the m smallest eigen-values corresponding to the buckling modes

$$\lambda_{1...m} > r^l \tag{29}$$

where the bound r^l may include some safety margin.
The force- or strain-based failure criteria are recast into failure indices

$$f = r_k / r_k^{l,u} \tag{30}$$

where the physical response r_k is bounded by $r_k^{l,u}$. The failure index is subjected to a bound $f \leq f_u$ with f_u being typically 1, or a knocked-down bound to include a factor of safety.

4. Skin Panel Models of CRM Wing

The structural optimization studies in this paper are performed on the NASA Common Research Model (CRM) [20], specifically on a structural model of the CRM wing generated at the DLR - Institute of Aeroelasticity [21], under the configuration name FERMAT. The FE model of the full aircraft and the wing are shown in Figure 3. The structural model comprises of shell and beam elements, with homogenized membrane, bending and transverse shear stiffness terms for the shell elements in the skin.

4.1 Sub-models of skin panels

In the present paper, optimization studies are performed on skin panels of the wing in order to observe performance trends between sandwich and monolithic composite designs. A skin panel is defined as the intersection between two ribs and spars.
In order to create these skin panel sub-models the following approach is followed.

- A trim calculation is performed on the full aircraft model for the following load-case: $+2.5g$ pull-up, Mach number $Ma = 0.57$, flight level 0 and maximum take-off weight (MTOW) corresponding to $260t$. This load-case was selected from a preliminary check of the element stresses arising out of different potential load-cases. In principle, any other flight condition, preferably a dominant one for sizing, could also be used for this study.

- A nodal force balance is used to calculate the forces to be applied on an isolated skin panel, in order that the panel exhibits the same loaded state as in the full-wing. These nodal forces are applied along the edge of the panel.

- The isolated skin panel is assumed to have simply-supported boundary conditions as shown in Figure 4, for analyses to be carried out on the sub-model level.

As a check, it was seen that the stress distribution in the isolated skin panel subjected to the extracted loads and boundary conditions, faithfully matches that of the panel in the full aircraft model. The applied loads on the skin panel are kept fixed during an optimization, rather than recalculating loads due to stress redistribution, in order to study each skin panel in an isolated setting.

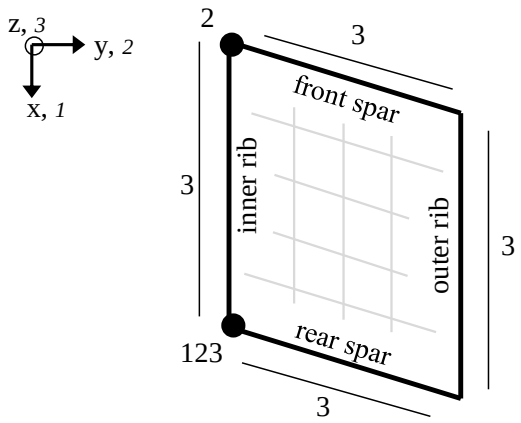

Figure 4 – Boundary conditions for the skin panel sub-model.

Table 1 – Material properties - Carbon-Epoxy Facesheets: *Hexcel IM7/8552 UD*.

Density (kg/m^3)	E_1	E_2 (GPa)	G_{12}	ν_{12}
1580	147.8	10.3	5.9	0.27

4.2 Material properties

For the monolithic laminates and facesheets in the sandwich composite, a carbon fibre - epoxy composite (IM7/8552) with the material properties listed in Table 1 is used.

Material failure in the composite laminate is accounted for using the AML approach. Failure strengths in compressions for different values of AML are obtained experimentally [40] as shown in Figure 5. The three curves represent the type of damage in the tested specimen: open-hole (OHC), filled-hole (FHC) and unnotched (UNC) compression.

In the present study, two types of honeycomb materials for the sandwich core are studied: HRH10 Nomex (Aramid) and 5052-Aluminium. Both are mid-specification materials readily available off-the-shelf, the former suitable for lightly-loaded segments of the wing, with the latter offering much higher material strengths. Since honeycomb are not expected to carry in-plane loads, their in-plane stiffness parameters E_1, E_2 and G_{12} are nominally set close to zero. The other relevant properties [41] are listed in Table 2. The properties of the honeycomb material are anisotropic in nature, arising from the different characteristics along the direction of the ribbon (denoted by L) and transverse to the ribbon direction (denoted by W). The principal material axis for both the facesheet and the core is oriented along the front spar, such that directions 1 (in the composite 1-2 orientation system) and

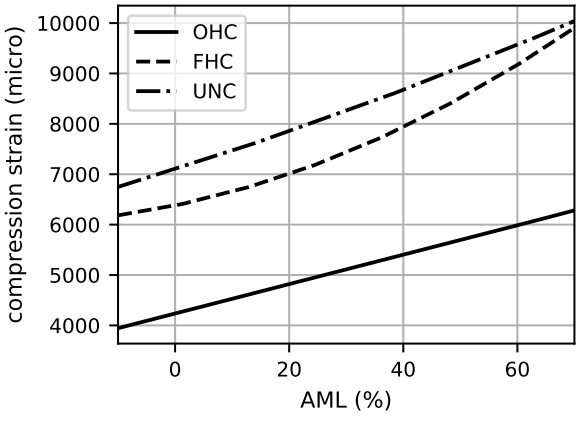

Figure 5 – Variation of allowable strains with AML for IM7/8552 composite - NIAR [40].

Table 2 – Material properties of honeycomb core material [41].

Density (kg/m^3)	Cell size (mm)	E_z	G_{Lz}	S_{Lz}	G_{Wz}	S_{Wz}
			(MPa)			
Hexcel-HRH10 Nomex (Aramid)						
64	3	190.0	63.0	2.0	35.0	1.0
5052 Aluminium						
72	3	1034.0	483.0	2.3	214.0	1.5

Table 3 – Optimization summary.

Optimization objective	*min* (structural weight)
Optimization constraints	
feasibility	LP-space constraints [38]
	Balance
	Standard angles $(0°, 90°, \pm 45°)$
	Angle fractions, $v_0, v_{90}, v_{\pm 45} > 0.1$
physical	buckling, $\lambda > 1.5$
	AML, $f_{AML} \leq 0.67$
physical	wrinkling, $f_{wrink} \leq 0.67$
(sandwich-specific)	crimping, $f_{crimp} \leq 0.67$
	dimpling, $f_{dimp} \leq 0.67$
	core-shear, $f_{cshear} \leq 0.67$
Design variables	
monolithic design	t, ξ^A_{1-4}, ξ^D_{1-4}
sandwich design	t_f, t_c , ξ^A_{1-4}, ξ^D_{1-4}, ξ^{Bu}_{1-4}

L (in the core L-W orientation system) are along this material axis for the facesheet and core material respectively.

4.3 Summary of optimization objective and constraints

A summary of the optimization objective and constraints included in the following optimization study are presented in Table 3.

In the present studies, only the stiffness properties of the skin are optimized while those of the stringers are kept a constant. This was done in order to isolate performance comparisons between monolithic and sandwich composites in the skin. A more realistic study will simultaneously include stringer dimensions as optimization variables, as planned for future studies on the full wing. The stringer properties in the present case correspond to those obtained using a preliminary cross-sectional sizing tool used for pre-sizing the wingbox based on empirical methods.

The requirement on ultimate load through a safety factor of 1.5 over the limit loads is introduced directly on the physical constraints. The lower limit on the buckling factors is set to 1.5. For the strain- and force-based failure modes, their respect failure indices are set with an upper limit of $1/1.5$.

5. Results and Discussion

The results from the optimization study comparing monolithic composite structures with sandwich composites are presented in this section in Figure 6. For each of the skin panels, its sub-model is set up as described in Section 4.1 The nodal forces at the boundary nodes are scaled between 0.33 and 1.66 times the nominal load, which in this case corresponds to the nodal loads from a +2.5g pull-up manoeuvre as described in Section 4.1 This load scaling factor is chosen as an arbitrary parameter to visualize the various failure criteria over a wide range of loads. The normalized structural weight is plotted on the Y-axis, with the weight of the monolithic design corresponding to a loads scaling factor of 1.0 being used as the reference weight.

Each of the design points is also accompanied by a vector of failure indices. For a monolithic design, the vector represents the two failure modes: AML material failure and buckling respectively. For a sandwich design, the 6-element vector represents the failure modes in the order: AML strain failure, buckling, crimping, dimpling, wrinkling and core-shear respectively. A value lesser than 0 denotes feasibility of the failure index, while a value of 0 or larger denotes failure. The dominant failure mode at that design point is represented in bold font.

5.1 Skin panel near wing-tip

Considering the skin panel 1055 in Figure 3, right plot, the optimization trends between monolithic and sandwich composites are shown in Figure 6. The trend curves are with a sandwich composite comprising of a Nomex-Aramid core.

The outboard sections of the wing being lightly loaded, it is seen that buckling instability is the driving failure mode for the monolithic composite design. Sandwich composites are inherently superior in this very situation, being able to increase bending stiffness by adding core material, with low weight penalties. Consequently, for the loads scaling factor of 1.0, the skin panel with a sandwich composite design is $\sim 30\%$ lighter than its monolithic counterpart. The limiting factor here is the facesheet thickness required to withstand AML material failure and the core thickness required to tackle the sandwich-specific failure modes, shear crimping in this case.

Considering a core material having superior properties such as the Aluminium honeycomb in Table 2, similat weight trends are observed. With the significantly larger shear strengths and stiffness, the Aluminium-core sandwich composite is marginally better in performance compared to its Nomex-Aramid counterpart up to the limiting failure mode of AML, while offering larger failure margins for the sandwich failure modes. Moreover, a significantly smaller core thickness of $4mm$ is required for the former when compared with $8mm$ for the latter at the nominal loads scaling factor of 1.0. The studies henceforth use aluminium honeycomb for the sandwich composites.

The evolution of optimized thickness across the loads scaling factor is shown in Figure 7. At low load levels, core thickness is added in the sandwich design to counter failure due to buckling. At load levels higher than 0.66, AML becomes a driving criteria, with the facesheet thickness being increased while the added core thickness provides for the necessary bending stiffness to resist buckling.

Because sandwich composites offer a very large bending stiffness without penalizing structural weight, a potential strength of sandwich composites lies in the possibility of affording lesser number of stringers in the design. Stringers add geometric stiffness to the structure by reducing the dimensions of the buckling fields. Sandwich composites could require lesser stringers, thereby reducing manufacturing and maintenance costs over the structure's lifetime. In order to simulate such a scenario, 3 of the 4 stringers from this skin panel are removed as demonstrated in Figure 8.

The optimization trends corresponding to the skin panel 1055 with reduced number of stringers is shown in Figure 9. The mass of the monolithic design with the nominal number of stringers as in Figure 6 is used as the reference mass. With buckling being the dominant driver for the skin panel with the nominal number of stringers, a larger stringer pitch is detrimental to the monolithic design. Consequently the monolithic design is $\sim 40\%$ heavier due to the requirements of buckling. The sandwich design on the other hand, exhibits weight savings of about $\sim 25\%$ when compared to the nominal monolithic design.

This skin panel is however $\sim 5\%$ heavier than the sandwich skin panel with the nominal stringer pitch, due to weight being traded-off between the stringers and the skin in order to tackle the strain requirements of AML. In the end, a design choice could be made considering the structural weight, manufacturing and operating costs to arrive at a compromise on the design philosophy.

5.2 Discussion on mass savings on overall wing

In the full paper [19], weight studies on a skin-panel in the mid-span section of the wing and simulations considering improved material strengths have been presented. The studies show that a comparison between monolithic and sandwich composites is dependent on the segment of the wing considered, in particular, on the acting loads, which in turn dictates the driving failure mode. Potential weight savings by using sandwich composites can be conclusively reached after running optimization

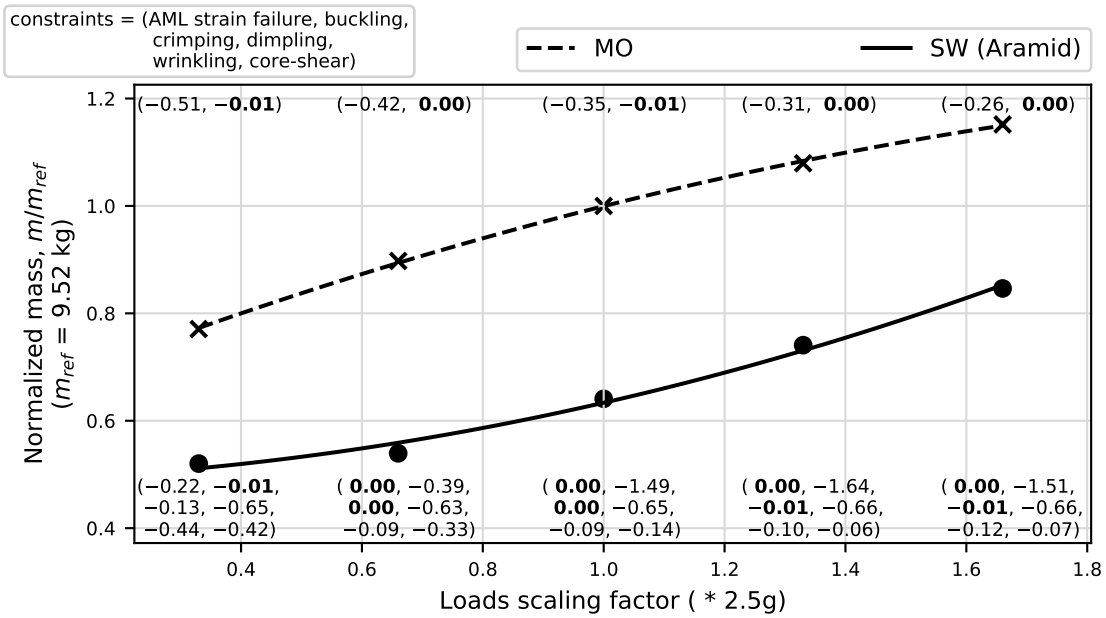

Figure 6 – Optimization trends comparing monolithic and sandwich designs for skin panel 1055.

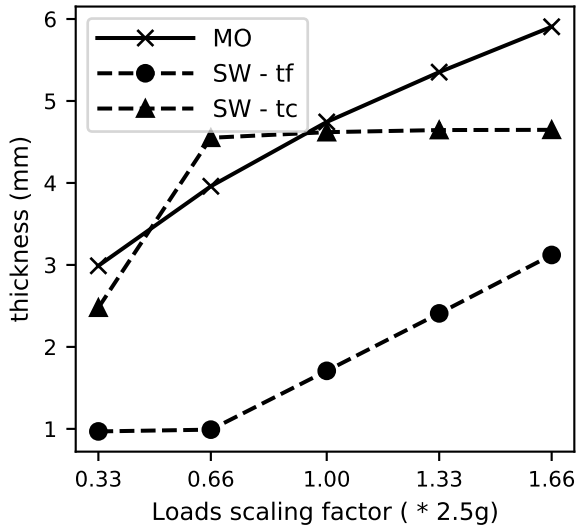

Figure 7 – Optimized thickness of monolithic laminate, sandwich facesheet, sandwich core for skin panel 1055.

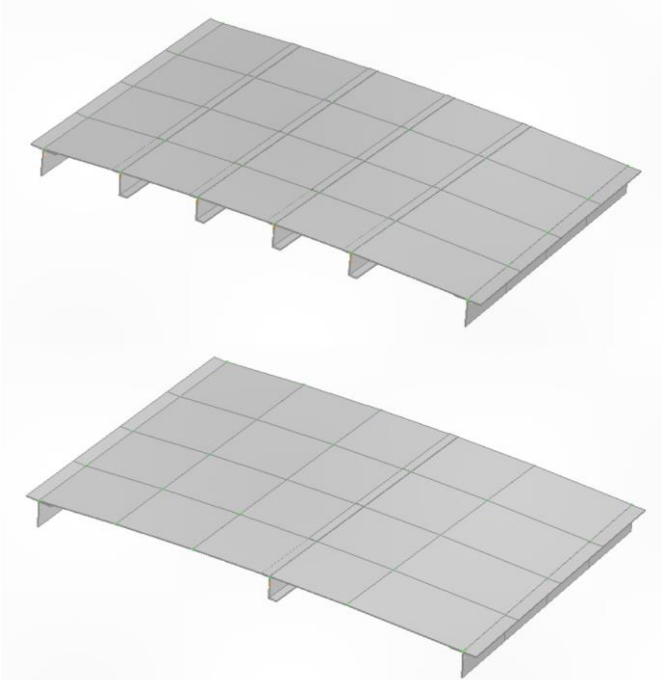

Figure 8 – Original skin panel 1055 (above) and skin panel with reduced stringers 1055 (v02) (below).

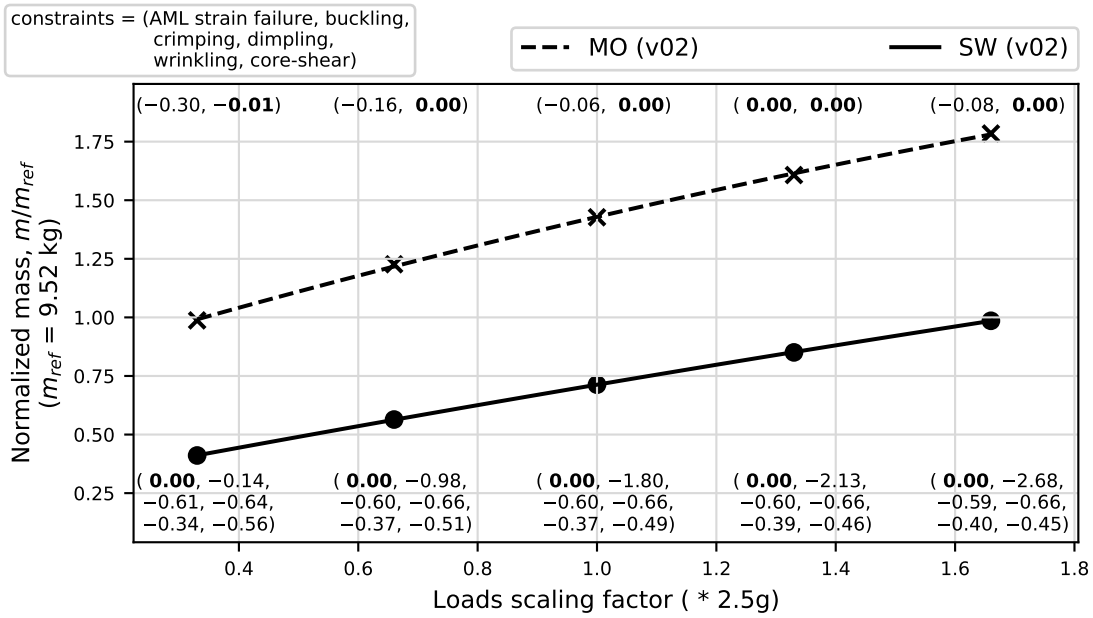

Figure 9 – Optimization trends comparing monolithic and sandwich (aluminium) designs for skin panel 1055 (v02).

studies on the full wing. The results from the above studies at the level of skin panels can nevertheless be indicative of performance metrics that can be achieved.
Assuming that savings in structural weight vary linearly from 25% in the outer-most skin panel to 0% in the skin panels near the mid-span, the cumulative weight savings in the upper skin in this segment alone translates to $\sim 10\%$. Weight saving with respect to the entire upper skin equates to $\sim 3\%$. The above values are estimated based on an available version of a composite CRM wing using empirical preliminary methods. Based on this model, proportional weight savings were calculated as a first estimate. This was done because a comprehensive composite version of the CRM wing did not exist at the time of writing of the present work.
The savings above could be conservative on account of two main reasons. Firstly, the use of sandwich composites would allow for a larger stringer pitch and possibly lesser number of stringers thereby reducing stringer weight in the full wing. Secondly, a reduction of mass in the out-board sections and the ensuing increase in structural flexibility could alleviate the bending moments along the entire wing when considering aeroelastic loads, which in turn would lead to weight savings also in in-board sections where sandwich composites are not necessarily used.
The CRM wing is inherently a heavily-loaded wing on account of the large span. A different reference wing that shows dominant buckling driven regions [1] could show significantly different results. With the methodology established and tested on a smaller scale example, carrying out detailed studies on full wing models would be a next step.

6. Conclusions and Outlook

A methodology for optimization of sandwich composite structures in preliminary wing design is presented in this work. The approach can be applied to the design of large-scale commercial-type wing applications. The failure modes exhibited by sandwich composites are addressed using conservative empirical formulae. Altogether, material failure through AML, buckling instability, facesheet wrinkling, shear crimping, facesheet dimpling and core-shear failure are accounted for. The continuous optimization step is addressed in this paper using a recently-developed lamination parameter scheme suited to sandwich composites. An optimization study is carried out on the skin panel sub-models of the CRM wing.
Depending on the span-wise section considered, skin panels with sandwich composite design exhibit weight savings of up to 30% when compared to the classic monolithic composite design. The trends show that when the skin panel is driven by buckling as a design requirement, sandwich composites outperform their monolithic counterparts on account of their higher bending stiffness to weight ratio. When material or strain-dominated criteria drive the design, sandwich composites offer a similar performance to monolithic skin panels. The study also showed that for lightly-loaded regions near the wing-tip, a larger stringer pitch can be afforded at low penalties to structural weight. This could potentially raise discussions on savings in manufacturing, maintenance and inspection costs.
In the next step, optimization studies will be carried out on the full CRM wing in order to better understand the performance gains achievable by using sandwich composites. The stringer pitch can also be better exploited to arrive at different optimal designs. The present studies show that in the CRM wing, the outer third of the wing structure might potentially be driven by buckling where sandwich composites would be the better choice. This of course might change when the stringer pitch is varied and ultimately, the question arises as to which configuration offers the optimal structural performance. Alternatively, a wing model with a lower span and aspect ratio can be considered given that the loading and thereby the strains would be lower and larger sections of the wing may be sized by buckling. The presented approach is well-suited to make precisely such studies.

7. Contact Author Email Address

mailto: Johannes.Dillinger@dlr.de

8. Copyright Statement

References

[1] Gustavo H. C. Silva, Alex Pereira do Prado, Pedro Higino Cabral, Roeland De Breuker, and Johannes K. S. Dillinger. Tailoring of a composite regional jet wing using the slice and swap method. *Journal of Aircraft*, 56(3):990–1004, May 2019.

[2] John H. Fogarty. Honeycomb core and the myths of moisture ingression. *Applied Composite Materials*, 17(3):293–307, June 2010.

[3] M.A. Stiftinger and F.G. Rammerstorfer. Face layer wrinkling in sandwich shells— theoretical and experimental investigations. *Thin-Walled Structures*, 29(1-4):113–127, September 1997.

[4] Linus Fagerberg. Wrinkling and compression failure transition in sandwich panels. *Journal of Sandwich Structures & Materials*, 6(2):129–144, March 2004.

[5] Linus Fagerberg and Dan Zenkert. Imperfection-induced wrinkling material failure in sandwich panels. *Journal of Sandwich Structures & Materials*, 7(3):195–219, May 2005.

[6] Erasmo Carrera. Theories and finite elements for multilayered plates and shells: a unified compact formulation with numerical assessment and benchmarking. *Archives of Computational Methods in Engineering*, 10(3):215–296, September 2003.

[7] Mauricio F. Caliri, Antonio J.M. Ferreira, and Volnei Tita. A review on plate and shell theories for laminated and sandwich structures highlighting the finite element method. *Composite Structures*, 156:63–77, November 2016.

[8] Lucien A. Schmit and Massood Mehrinfar. Multilevel optimum design of structures with fiber-composite stiffened-panel components. *AIAA Journal*, 20(1):138–147, January 1982.

[9] Mitsunori Miki and Yoshihiko Sugiyama. Optimum design of laminated composite plates using lamination parameters. In *32nd Structures, Structural Dynamics, and Materials Conference*, Baltimore,MD,U.S.A., April 1991. American Institute of Aeronautics and Astronautics.

[10] Srinivas Kodiyalam, Somanath Nagendra, and Joel DeStefano. Composite sandwich structure optimization with application to satellite components. *AIAA Journal*, 34(3):614–621, March 1996.

[11] Ching-Chieh Lin and Ya-Jung Lee. Stacking sequence optimization of laminated composite structures using genetic algorithm with local improvement. *Composite Structures*, 63(3-4):339–345, February 2004.

[12] Chongxin Yuan, Otto Bergsma, Sotiris Koussios, Lei Zu, and Adriaan Beukers. Optimization of sandwich composites fuselages under flight loads. *Applied Composite Materials*, 19(1):47–64, February 2012.

[13] Vladimir Balabanov, Olaf Weckner, Michael Epton, Gerald Mabson, Samuel Cregger, and Adriana Blom. Optimal design of a composite sandwich structure Using Lamination Parameters. In *53rd AIAA/ASME/ASCE/AHS/ASC Structures, Structural Dynamics and Materials Conference*, Honolulu, Hawaii, April 2012. American Institute of Aeronautics and Astronautics.

[14] Olaf Weckner and Vladimir Balabanov. Efficient design of shear-deformable hybrid composite structures, February 4 2014. US Patent 8,645,110.

[15] Peng Jin, Bifeng Song, Xiaoping Zhong, Tianxiang Yu, and Fei Xu. Aeroelastic tailoring of composite sandwich panel with lamination parameters. *Proceedings of the Institution of Mechanical Engineers, Part G: Journal of Aerospace Engineering*, 230(1):105–117, January 2016.

[16] Gunther Moors, Christos Kassapoglou, Sergio Frascino Müller de Almeida, and Clovis Augusto Eça Ferreira. Weight trades in the design of a composite wing box: effect of various design choices. *CEAS Aeronautical Journal*, 10(2):403–417, June 2019.

[17] Gustavo H. C. Silva and Yasser Meddaikar. Lamination parameters for sandwich and hybrid material composites. *AIAA Journal*, pages 1–8, July 2020.

[18] François-Xavier Irisarri, Cédric Julien, Dimitri Bettebghor, Florian Lavelle, Yannick Guerin, and Kevin Mathis. A general optimization strategy for composite sandwich structures. *Structural and Multidisciplinary Optimization*, February 2021.

[19] Yasser M. Meddaikar, Johannes K. S. Dillinger, Gustavo H. C. Silva, and Roeland De Breuker. Skin panel optimization of the common research model wing using sandwich composites. 59(2):386–399.

[20] John C. Vassberg, Mark A. DeHaan, Melissa S. Rivers, and Richard A. Wahls. Retrospective on the Common Research Model for computational fluid dynamics validation studies. *Journal of Aircraft*, 55(4):1325–1337, July 2018.

[21] Thomas Klimmek. Parametric set-up of a structural model for FERMAT configuration for aeroelastic and loads analysis. *Journal of Aeroelasticity and Structural Dynamics*, (2):31–49, May 2014.

[22] J. K. S. Dillinger, T. Klimmek, M. M. Abdalla, and Z. Gürdal. Stiffness optimization of composite wings with aeroelastic constraints. *Journal of Aircraft*, 50(4):1159–1168, July 2013.

[23] Design and analysis of sandwich structures. In *Composite Materials Handbook – 17*, volume 6, chapter 4, pages 1–228. SAE International, Wichita, Kansas, July 2017.

[24] Paolo Feraboli. Composite materials strength determination within the current certification methodology for aircraft structures. *Journal of Aircraft*, 46(4):1365–1374, July 2009.

[25] *MSC Nastran 2017 Quick Reference Guide*. MSC Software Corp, 2017.

[26] Christos Kassapoglou. *Design and analysis of composite structures: with applications to aerospace structures*. John Wiley & Sons Ltd, Oxford, UK, May 2013.

[27] N. J. Hoff and S. E. Mautner. The buckling of sandwich-type panels. *Journal of the Aeronautical Sciences*, 12(3):285–297, July 1945.

[28] Dan Zenkert and Nordisk Industrifond, editors. *The handbook of sandwich construction*. North European engineering and science conference series. Engineering Materials Advisory Services Ltd. (EMAS), Cradley Heath, West Midlands, 1997. OCLC: 246395327.

[29] J. Enrique Herencia, Paul M. Weaver, and Michael I. Friswell. Optimization of long anisotropic laminated fiber composite panels with T-shaped stiffeners. *AIAA Journal*, 45(10):2497–2509, October 2007.

[30] J. Enrique Herencia, Raphael T. Haftka, Paul M. Weaver, and Michael I. Friswell. Lay-Up optimization of composite stiffened panels using linear approximations in lamination space. *AIAA Journal*, 46(9):2387–2391, September 2008.

[31] Samuel T. IJsselmuiden, Mostafa M. Abdalla, Omprakash Seresta, and Zafer Gürdal. Multi-step blended stacking sequence design of panel assemblies with buckling constraints. *Composites Part B: Engineering*, 40(4):329–336, June 2009.

[32] Francois-Xavier Irisarri, Mostafa M. Abdalla, and Zafer Gürdal. Improved Shepard's method for the optimization of composite structures. *AIAA Journal*, 49(12):2726–2736, December 2011.

[33] Dianzi Liu and Vassili V. Toropov. A lamination parameter-based strategy for solving an integer-continuous problem arising in composite optimization. *Computers & Structures*, 128:170–174, November 2013.

[34] Dianzi Liu, Vassili V. Toropov, David C. Barton, and Osvaldo M. Querin. Weight and mechanical performance optimization of blended composite wing panels using lamination parameters. *Structural and Multidisciplinary Optimization*, 52(3):549–562, September 2015.

[35] Yasser M. Meddaikar, François-Xavier Irisarri, and Mostafa M. Abdalla. Laminate optimization of blended composite structures using a modified Shepard's method and stacking sequence tables. *Structural and Multidisciplinary Optimization*, 55(2):535–546, February 2017.

[36] M. Autio. Determining the real lay-up of a laminate corresponding to optimal lamination parameters by genetic search. *Structural and Multidisciplinary Optimization*, 20(4):301–310, December 2000.

[37] F.-X. Irisarri, A. Lasseigne, F.-H. Leroy, and R. Le Riche. Optimal design of laminated composite structures with ply drops using stacking sequence tables. *Composite Structures*, 107:559–569, January 2014.

[38] Masaki Kameyama and Hisao Fukunaga. Optimum design of composite plate wings for aeroelastic characteristics using lamination parameters. *Computers & Structures*, 85(3-4):213–224, February 2007.

[39] Terence Macquart, Marco T. Bordogna, Paul Lancelot, and Roeland De Breuker. Derivation and application of blending constraints in lamination parameter space for composite optimisation. *Composite Structures*, 135:224–235, January 2016.

[40] K. Marlett. Hexcel 8552 IM7 unidirectional prepreg 190 gsm & 35%RC qualification material property data report. Technical Report CAM-RP-2009-015 Rev A, National Institute for Aviation Research, Wichita, KS, April 2011.

[41] Hexcel. Honeycomb sandwich design technology - Hexcel, 2000.